Physics of the Solid State, Vol. 44, No. 6, 2002, pp. 1077–1084. Translated from Fizika Tverdogo Tela, Vol. 44, No. 6, 2002, pp. 1032–1038.

SEMICONDUCTORS AND DIELECTRICS

Mechanism of Protonic Conductivity in an NH_4HSeO_4 Crystal

Yu. N. Ivanov*, A. A. Sukhovsky*, I. P. Aleksandrova*, J. Totz, and D. Michel****

** Kirensky Institute of Physics, Siberian Division, Russian Academy of Sciences, Akademgorodok, Krasnoyarsk, 660036 Russia*

*** Leipzig University, D04103 Leipzig, Germany*

e-mail: rsa@iph.krasn.ru

Received July 20, 2001; in final form, October 25, 2001

Abstract—The chemical exchange of deuterons in a partly deuterated ammonium hydrogen selenate crystal is investigated by deuteron magnetic resonance (^{2}H NMR) spectroscopy over a wide range of temperatures. The changes observed in the line shape of the NMR spectra at temperatures above 350 K are characteristic of chemical exchange processes. The exchange processes are thoroughly examined by two-dimensional ^{2}H NMR spectroscopy. It is established that, over the entire temperature range, only deuterons of hydrogen bonds are involved in the exchange and the rates of exchange between deuterons of all types are nearly identical. No deuteron exchange between the ND_4 groups and hydrogen bonds is found. A new model of proton transport in ammonium hydrogen selenate is proposed on the basis of the experimental data. This model makes it possible, within a unified context, to explain all the available experimental data, including macroscopic measurements of the electrical conductivity. © *2002 MAIK "Nauka/Interperiodica".*

1. INTRODUCTION

Considerable recent interest expressed by researchers in crystals with a high ionic conductivity stems from both important practical applications of these compounds and the basic problems concerning electrical conductivity in superionic crystals [1–4]. In this respect, crystals whose structure involves quasi-one-dimensional chains of hydrogen bonds are of particular importance. These crystals are good model objects for use in verifying different assumptions on microscopic mechanisms of ionic conductivity. Ammonium hydrogen selenate (AHS) NH_4HSeO_4 belongs to these crystals. In the structure of AHS crystals, infinite quasi-one-dimensional chains are formed by SeO_4 tetrahedra joined through protons of hydrogen bonds. The deuteration of AHS makes it possible to apply the powerful method of nuclear magnetic resonance (NMR) at quadrupole nuclei to perform research into proton (deuteron) transport. In addition to conventional Fourier-transform NMR spectroscopy, elementary processes of deuteron chemical exchange have been investigated by two-dimensional (2*D*) NMR spectroscopy. As a rule, the 2*D* NMR data are compared with the results of dielectric measurements performed over a wide range of frequencies (10^{-2}–10^6 Hz). Dielectric measurements at very low frequencies permit one to increase appreciably the accuracy in determination of the dc conductivity σ_{dc} and to compare quantitatively the results of dielectric and NMR measurements for AHS crystals. The structure and properties of AHS single crystals have been described thoroughly in our earlier works [4–7]. In the present work, we analyzed our results with the aim of elucidating the microscopic mechanism of proton transport in AHS crystals.

2. SAMPLE PREPARATION AND EXPERIMENTAL TECHNIQUE

Partly deuterated (25%) AHS crystals were grown from an aqueous solution containing an excess of H_2SeO_4 and the appropriate amount of heavy water. Protons involved both in ammonium groups and in hydrogen bonds were partly replaced by deuterons. The degree of deuteration was chosen reasoning from the specific features of the phase diagram of the NH_4HSeO_4 compound, which, at a growth temperature of 30°C and a degree of deuteration higher than 45%, crystallizes in another phase [8]. The nuclear magnetic resonance and dielectric measurements were performed with the same samples. The ^{2}H NMR investigations were carried out on a BRUKER MSL 300 NMR spectrometer operating at a Larmor frequency of 46.073 MHz. The width of a 90° pulse was equal to approximately 4 μs. A spin echo sequence with a time interval of 25 μs between pulses was used in order to exclude the effect of the dead time of the NMR spectrometer receiver. Moreover, proton decoupling was applied to suppress the broadening of ^{2}H NMR lines due to the dipole–dipole interaction with the remaining protons. The two-dimensional NMR measurements were performed using the following spin echo sequence: $(\pi/2)_x$–t_1–$(\pi/2)_{-x}$–τ_m–$(\pi/2)_x$–τ–$(\pi/2)_y$–τ–t_2, where t_1 is the evolution time, t_2 is the measurement

time, τ is the time interval between pulses, and τ_m is the mixing time. The dielectric susceptibility was measured on a Schlumberger Solartron 1255 HF Frequency Response Analyzer in the frequency range from 10^{-2} to 10^6 Hz. Samples approximately 0.8 mm thick were cut from the AHS single crystal. For dielectric measurements, electrodes were prepared in the form of thin gold films applied to the sample surface under vacuum.

3. RESULTS AND DISCUSSION

The most interesting features inherent in the AHS crystal are as follows: the ferroelectric state associated with ordering of protons involved in hydrogen bonds, the incommensurate phase [6, 7], and the protonic conductivity [1–3]. In the paraelectric phase, the AHS crystal is characterized by a monoclinic unit cell with space group $B2$ and the lattice parameters a = 19.745 Å, b = 4.611 Å, c = 7.552 Å, and γ = 102.56° [9]. The crystal structure is built up of SeO_4^{2-} tetrahedral ions joined by hydrogen bonds into infinite chains aligned along the ferroelectric axis **b** (Fig. 1). The SeO_4 groups are linked by ammonium ions along the two other axes **a** and **c**. Hydrogen bonds between the different structural groups SeO_4 considerably differ from each other. The length of the hydrogen bonds between the $Se(1)O_4$ groups (α bonds) is equal to 2.56 Å, and the length of the hydrogen bonds between the $Se(2)O_4$ groups (β bonds) is 2.59 Å (Fig. 1). In the paraelectric phase, protons of the α bonds are disordered dynamically [6, 7]. Reasoning from the analysis of the ^{1}H NMR spectra and measurements of the ^{1}H spin–lattice relaxation time, Moskvich *et al.* [1] assumed that the isotropic diffusive motion of ammonium groups and protons of hydrogen bonds occurs in the paraelectric phase. These authors proposed a microscopic mechanism of proton transport through a correlated reorientation of SeO_4 groups with a sequential exchange of protons between SeO_4 groups along an infinite chain of hydrogen bonds. In this case, the activation energy for reorientational motion of SeO_4 groups is a controlling factor of the proton hopping rate. It should be noted that the activation energy for reorientational motion of SeO_4 groups is approximately equal to the activation energy for isotropic diffusion of ammonium groups which contribute significantly to the electrical conductivity of the crystal [1, 2]. However, for the most part, all these assumptions are based on analyzing the temperature dependence of the second moment (linewidth) of the ^{1}H NMR spectra. It is known that, over the entire temperature range, the ^{1}H NMR spectrum consists of a single line whose second moment is predominantly determined by the dipole–dipole interactions between protons of ammonium groups [1]. In our opinion, these investigations cannot provide detailed information on the microscopic mechanism of proton transport in the AHS crystal.

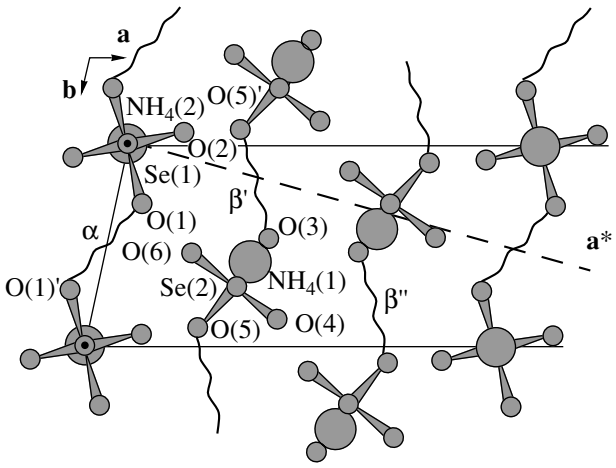

Fig. 1. Structure of NH_4HSeO_4 in the paraelectric phase. A half of the unit cell is shown. Wavy lines indicate hydrogen bonds between the oxygen atoms of the SeO_4 groups.

In this work, the microscopic characteristics of ammonium hydrogen selenate are determined from the ^{2}H NMR spectra of a partly deuterated AHS crystal. Unlike protons, deuterium nuclei possess a quadrupole moment. Nuclear magnetic resonance at quadrupole nuclei provides valuable information on the magnitude and symmetry of crystal-electric-field gradients at the studied nucleus. For a strong external magnetic field $\mathbf{B}_0$, when the Zeeman interaction energy substantially exceeds the energy of interaction between the nuclear quadrupole moment and the crystal field, the crystal field brings about a perturbation of equidistant Zeeman levels and a splitting of the NMR line into $2I$ components (I is the nuclear spin), which are symmetrically located with respect to the Larmor precession frequency ν_0 in the magnetic field $\mathbf{B}_0$ [10]. Consequently, the NMR spectrum of deuterons (I_D = 1) consists of doublets whose number for a single-crystal sample in the general case is equal to the number of magnetically nonequivalent deuterium nuclei. According to Pound [10], the quadrupole splitting ($\nu_2 - \nu_1$) can be represented by the relationship

$$\nu_2 - \nu_1 = \frac{6eQ}{4h} V_{zz}^{LAB} = \Phi_{zz}, \qquad (1)$$

where Q is the nuclear quadrupole moment, e is the elementary charge, h is the Planck constant, and V_{zz} is the zth component (the magnetic field $\mathbf{B}_0$ is aligned along the **z** axis) of the electric-field gradient at the nucleus. All the components V_{ij} of the electric-field gradient tensors for each structurally nonequivalent position of deuterium in the crystal in the laboratory coordinate system can be determined from the orientation dependences of the quadrupole splitting within the framework of the well-known Volkoff method [11]. The elec-

tric-field gradient tensor (for simplicity, the values of Φ_{ij} in frequency units will be used instead of V_{ij})—a symmetric second-rank tensor with zero spur—accounts for the point symmetry at the position of the nucleus under investigation. Specifically, for the α- and β-type hydrogen bonds in the AHS crystal, the principal axis Φ_{33} of the electric-field gradient tensor approximately coincides with the direction of the O–H···O hydrogen bond and the principal axis Φ_{22} is perpendicular to the plane of the Se–O···O bond. On this basis, each electric-field gradient tensor can be assigned to a particular hydrogen bond in the crystal. Thus, the magnetic resonance at ^{2}H nuclei in a partly deuterated AHS crystal appreciably extends the capabilities of the NMR technique and makes it possible to determine the individual dynamic characteristics of protons involved in hydrogen bonds and ammonium groups.

Figure 2 displays typical temperature dependences of the ^{2}H NMR spectra for an AHS crystal in the range 300–400 K. These spectra were measured for a crystal orientation at which the **b** axis is perpendicular to the external magnetic field $\mathbf{B}_0$ and the angle between the **a*** axis and the field $\mathbf{B}_0$ is equal to 15°. For this orientation, the ^{2}H NMR spectra contain two groups of lines. The central doublets (Fig. 2a) are assigned to the deuterons of the ammonium groups, and three doublets with splittings larger than 20 kHz (Fig. 2b) are attributed to the deuterons of the hydrogen bonds. As is clearly seen from Fig. 2a, no significant changes occur in the central portion of the spectrum over the entire temperature range of the existence of the paraelectric phase. Two electric-field gradient tensors for the deuterons of the ammonium groups (Table 1) were determined from the angular dependences of the ^{2}H NMR spectra at temperatures T = 300 and 390 K. One tensor is similar to an axially symmetrical tensor and corresponds to the deuterons of the ammonium groups in special positions. The other tensor is assigned to the deuterons of the ammonium groups in general positions. The small quadrupole coupling constant for these deuterons indicates a fast reorientation of the ammonium groups in the paraelectric phase. Therefore, in this case, the parameters of the electric-field gradient tensor account for an effective distortion of the ammonium group due to its environment. As follows from Table 1, an increase in the temperature leads to an insignificant change in the parameters of both electric-field gradient tensors in the paraelectric phase of the AHS crystal. These findings unambiguously demonstrate the absence of chemical exchange between two structurally nonequivalent ammonium groups over the entire range of the existence of the paraelectric phase. Consequently, the hypothesis proposed in [1] regarding isotropic diffusion of ammonium groups at 390 K should be revised. Analysis of the second moments of the ^{2}H NMR lines broadened at the expense of dipole–dipole interactions (hereafter, these lines will be referred to as the dipole-broadened lines) gives results that are in agreement with the

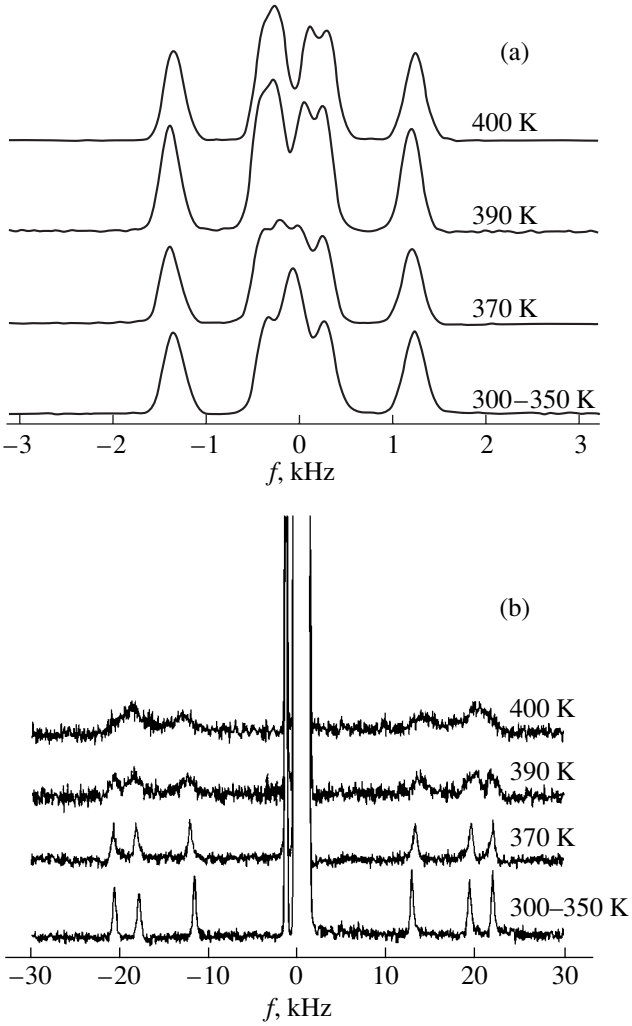

Fig. 2. Temperature dependences of the ^{2}H NMR spectra of an AHS crystal in the paraelectric phase: (a) the central quadrupole doublets assigned to the deuterons of the ammonium groups and (b) the side peaks attributed to the deuterons of the hydrogen bonds. The spectra are measured for a crystal orientation with the **b** axis perpendicular to the external magnetic field $\mathbf{B}_0$. The angle between the **a*** axis and the field $\mathbf{B}_0$ is equal to 15°.

aforementioned data and provides additional information on the deuteron motion. The dominant contribution to the width of the ^{2}H NMR lines assigned to the ammonium groups is made by the intermolecular dipole–dipole interaction of the ammonium deuterons with each other and the dipole–dipole interaction of the ammonium deuterons with deuterons of the hydrogen bonds. The dipole broadening of the ^{2}H NMR lines due to the dipole interaction of the deuterons with the remaining protons is suppressed by proton decoupling, whereas the intramolecular dipole interactions of the deuterons involved in the ammonium groups are averaged through fast reorientation of these groups. Taking into account the deuterons (with due regard for the

Table 1. Parameters of the electric-field gradient tensors for two structurally nonequivalent ammonium groups in the AHS crystal

Temperature, K	$NH_4(1)$				$NH_4(2)$			
	principal values of electric-field gradient tensors Φ_{ii}, Hz	direction cosines (magnitudes) with respect to crystallographic axes			principal values of electric-field gradient tensors Φ_{ii}, Hz	direction cosines (magnitudes) with respect to crystallographic axes		
		a*	**b**	**c**		**a***	**b**	**c**
300	$\Phi_{11} = -1196$	0.51	0.77	0.39	$\Phi_{11} = -1350$	0	0	1
	$\Phi_{22} = -402$	0.4	0.61	0.68	$\Phi_{22} = -1329$	0.73	0.68	0
	$\Phi_{33} = 1598$	0.76	0.19	0.62	$\Phi_{33} = 2679$	0.68	0.73	0
390	$\Phi_{11} = -920$	0.26	0.93	0.26	$\Phi_{11} = -850$	0	0	1
	$\Phi_{22} = -519$	0.47	0.35	0.81	$\Phi_{22} = -1306$	0.72	0.69	0
	$\Phi_{33} = 1439$	0.84	0.09	0.53	$\Phi_{33} = 2156$	0.69	0.72	0

Table 2. Theoretical (calculated with inclusion of all the magnetic nuclei, except for protons, and a random distribution of deuterons) and experimental (at 300 K) second moments of the ^2H NMR lines attributed to the ammonium groups in the AHS crystal

Orientation of field $\mathbf{B}_0$	Group $NH_4(1)$		Group $NH_4(2)$	
	M_2, Hz^2		M_2, Hz^2	
	Calculation	Experiment	Calculation	Experiment
$\|\|\mathbf{a}^*$	1.95×10^4	$(2 \pm 0.2) \times 10^4$	1.58×10^4	$(1.7 \pm 0.2) \times 10^4$
$\|\|\mathbf{b}$	1.96×10^4	$(2 \pm 0.2) \times 10^4$	1.81×10^4	$(2 \pm 0.2) \times 10^4$
$\|\|\mathbf{c}$	1.5×10^4	$(1.7 \pm 0.2) \times 10^4$	1.1×10^4	$(1.2 \pm 0.2) \times 10^4$

Table 3. Theoretical (calculated as described in Table 2, except for the contribution of the dipole–dipole interaction between the deuterons of ammonium groups and the deuterons of hydrogen bonds) and experimental (at 390 K) second moments of the ^2H NMR lines attributed to the ammonium groups in the AHS crystal

Orientation of field $\mathbf{B}_0$	Group $NH_4(1)$		Group $NH_4(2)$	
	M_2, Hz^2		M_2, Hz^2	
	calculation	experiment	calculation	experiment
$\|\|\mathbf{a}^*$	6.89×10^3	$(1.0 \pm 0.2) \times 10^4$	6.72×10^3	$(0.9 \pm 0.2) \times 10^4$
$\|\|\mathbf{b}$	1.5×10^4	$(1.6 \pm 0.2) \times 10^4$	1.48×10^4	$(1.6 \pm 0.2) \times 10^4$
$\|\|\mathbf{c}$	7.61×10^3	$(1.0 \pm 0.2) \times 10^4$	7.63×10^3	$(0.9 \pm 0.2) \times 10^4$

degree of deuteration) and other magnetic nuclei, except for protons, we calculated the second moments of the ^2H NMR lines. The lattice sums were calculated in a sphere of radius 40 Å. The calculated second moments are in agreement with the experimental data at 300 K (Table 2). An increase in the temperature leads to a decrease in the experimental second moments of the ^2H NMR lines associated with the ammonium groups (Table 3). It is interesting to note that the experimental second moments at 390 K agree well with the theoretical moments calculated without regard for the dipole interaction with the deuterons of the hydrogen bonds. This suggests a fast diffusive motion of these protons (deuterons). More detailed information can be obtained from analyzing the relevant lines of the NMR spectra.

It can be seen from Fig. 2b that the side components of the NMR spectra do not exhibit noticeable changes in the temperature range from 300 to 350 K. The parameters of two electric-field gradient tensors for two structurally nonequivalent positions of the protons involved in the α- and β-type hydrogen bonds were cal-

culated from the orientation dependences of the quadrupole splittings at 300 K. The results of calculations coincide with the data obtained in our earlier work [12]. At temperatures above 350 K, the side components of the NMR spectrum become broadened (Fig. 2b). This indicates that chemical exchange occurs in a system of hydrogen bonds in the crystal. However, the contribution of this exchange is substantially less than the quadrupole splitting up to the temperature of phase transition to the superionic phase (417 K). Hence, the mechanism of proton motion cannot be judged from these spectra. It is only possible to estimate the rate of chemical exchange from the NMR linewidth in the framework of the well-known Anderson theory (see, for example, [13]). The calculated rates of chemical exchange are as follows: 0.5×10^3 s^{-1} at 370 K, 2×10^3 s^{-1} at 390 K, and 4×10^3 s^{-1} at 400 K. In order to obtain information on the microscopic mechanism of the deuteron mobility, the exchange rate, and the activation energy of this process, we used two-dimensional ^{2}H NMR spectroscopy. The mathematical formalism of the chemical exchange processes and numerical calculations of the exchange rates from two-dimensional NMR spectra have been described in a number of well-known works [14, 15]. Here, we outline this method only briefly. The exchange kinetics, as a rule, is characterized by the probability (rate) p_{ij} of transferring an atom from the position i to the position j in a unit time. The chemical exchange can be represented by the basic equation (see, for example, [13])

$$\frac{\partial n_i}{\partial t} = \sum_j^n p_{ij} n_j \qquad (2)$$

or, in the matrix form, as $\dot{\mathbf{n}} = \mathbf{pn}$ with the solution

$$\mathbf{n}(t) = \exp(\mathbf{p} \cdot t)\mathbf{n}_0 = A(t)\mathbf{n}_0. \qquad (3)$$

Here, the components n_{0i} of the vector $\mathbf{n}_0\{n_{01}, \ldots, n_{0i}\}$ are equal to the number of deuterons at the ith position at the instant of time $t = 0$ and the components n_i of the vector $\mathbf{n}(t) = \{n_1, \ldots, n_i\}$ are equal to the number of deuterons at the same position at the instant $t = \tau_m$. The components $A_{ij}(t)$ of the exchange matrix $A(t)$ in relationship (3) completely determine the kinetics of deuteron (proton) exchange in the crystal and can be obtained from the intensities of the corresponding peaks in the two-dimensional ^{2}H NMR spectra [14, 15]. In our recent work [4], the AHS crystal was thoroughly investigated by two-dimensional ^{2}H NMR spectroscopy. Here, we present only the results that are essential to the understanding of the microscopic mechanism of protonic conductivity. The two-dimensional ^{2}H NMR experiments with the AHS crystal were performed in the temperature range 300–350 K. Figure 3 shows the left upper quadrant of the typical total two-dimensional ^{2}H NMR spectrum of the AHS crystal (at a temperature of 350 K and a mixing time of 3 ms). These spectra

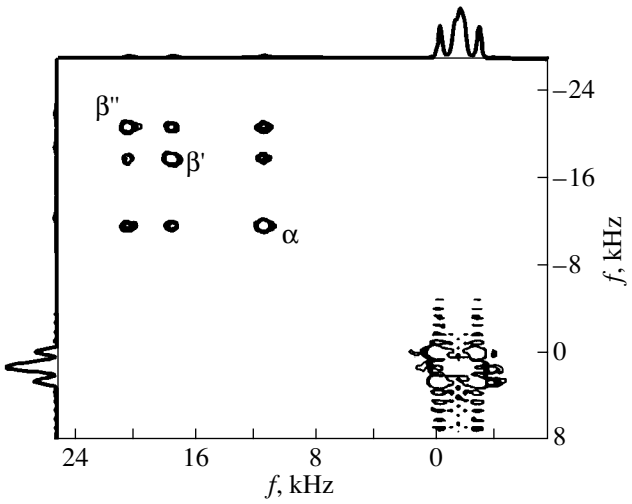

Fig. 3. Two-dimensional ^{2}H NMR exchange spectrum of the AHS crystal at a temperature of 350 K and a mixing time of 3 ms (only the upper left quadrant is shown). The crystal orientation is the same as in Fig. 2. The exchange is characterized by the off-diagonal peaks and occurs between deuterons at the positions α, β', and β".

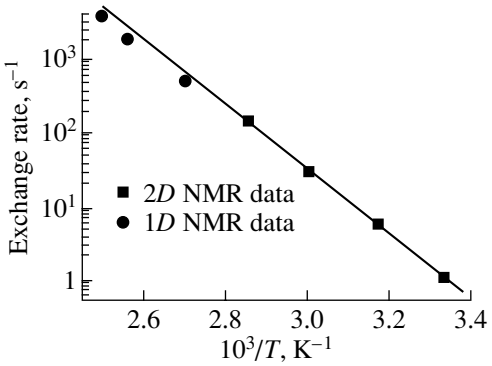

Fig. 4. Temperature dependence of the deuteron exchange rate for an AHS crystal according to 1*D* and 2*D* NMR data. $E_a = 81.1$ kJ mol^{-1} and $p_0 = 1.9 \times 10^{14}$ s^{-1}.

were measured at the same orientation as for the one-dimensional (1*D*) ^{2}H NMR spectra displayed in Fig. 2. The typical off-diagonal peaks (see, for example, [14, 15]) in Fig. 3 indicate deuteron exchange between hydrogen bonds of two types (the α and β bonds) and between magnetically nonequivalent positions of the adjacent bonds. Note that the rates of these processes are approximately equal to each other. The two-dimensional NMR spectra unambiguously demonstrate that no chemical exchange between the deuterons of the ammonium groups and the deuterons of the hydrogen bonds occurs over the entire temperature range of the existence of the paraelectric phase. Figure 4 depicts the temperature dependence of the exchange rate according

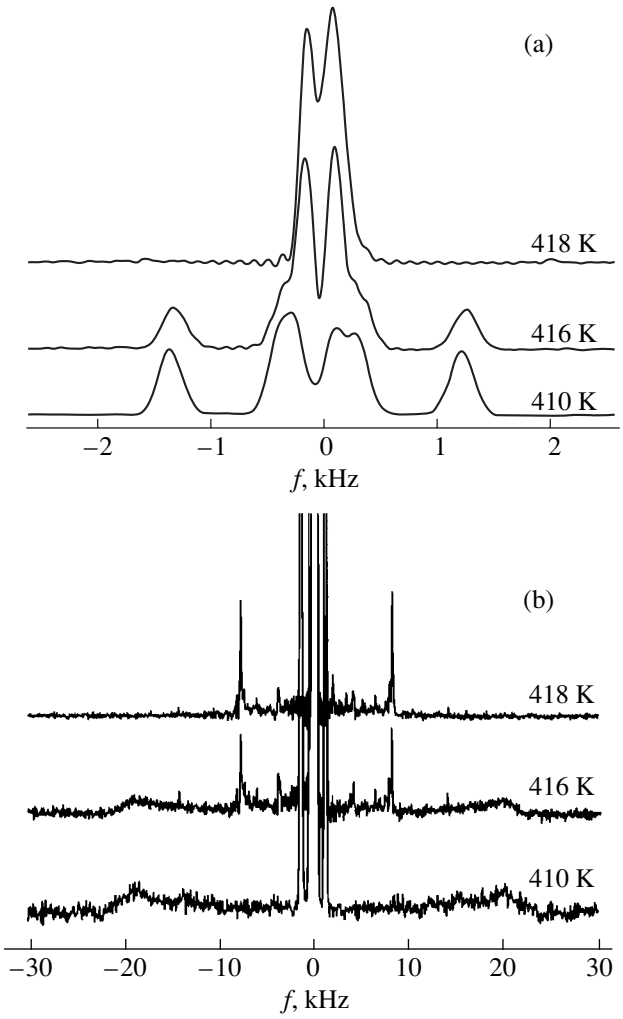

Fig. 5. Temperature dependences of the ^{2}H NMR spectra of an AHS crystal in the vicinity of the phase transition to the superionic state: (a) the central quadrupole doublets assigned to the deuterons of the ammonium groups and (b) the side peaks attributed to the deuterons of the hydrogen bonds. The crystal orientation is the same as in Fig. 2.

to the data of one-dimensional and two-dimensional NMR spectroscopy. The solid line in Fig. 4 represents the approximation of this dependence by the Arrhenius equation with the activation energy E_a:

$$p(T) = p_0 \exp(E_a/RT). \quad (4)$$

It should be noted that the $2D$ ^{2}H NMR data and the estimates made from the $1D$ ^{2}H NMR spectra at high temperatures are in good agreement and lead to the following parameters of the exchange process: the activation energy is approximately equal to 80 kJ mol^{-1} and the preexponential factor is estimated as $p_0 = 1.9 \times 10^{14}$ s^{-1}. This suggests that the proton mobility in the paraelectric phase occurs through a sole mechanism, namely, through sequential hoppings of protons from one chain of hydrogen bonds to the adjacent chain. Therefore, the conductivity anisotropy in the AHS crystal should be insignificant. From the results of dielectric measurements [5], we determined the conductivity parallel and perpendicular to the crystallographic axis **b** (the direction of hydrogen bond chains). Within the limits of experimental error, no conductivity anisotropy is revealed in the temperature range from 300 to 350 K. For proton exchange, the activation energies determined from our NMR data and the temperature dependence of the conductivity coincide to within good accuracy [5]. At temperatures above 360 K, the conductivity for both directions deviates from the Arrhenius behavior toward larger values. It should be noted that these deviations vary from sample to sample for the same orientation. This can be explained by the high hygroscopicity of the AHS crystal. All the samples are characterized by a sharp increase in the conductivity upon transition to the superionic phase.

At 417 K, the AHS crystal undergoes a transition to the high-temperature superionic phase. Unfortunately, the crystal in this phase rapidly loses protons and is destroyed. For this reason, the superionic phase cannot be investigated thoroughly by nuclear magnetic resonance and diffraction methods. There exist only the assumptions that the superionic phase has the $P2/n$ [16] or $P2_1/b$ [17] symmetry. We analyzed the ^{2}H NMR spectra for several orientations of the AHS crystal in the temperature range 410–420 K. For each new orientation, we used a particular sample. Figure 5 displays the temperature dependences of the ^{2}H NMR spectra for the AHS crystal oriented in such a manner that the **b** axis is perpendicular to the external magnetic field $\mathbf{B}_0$ and the angle between the **a*** axis and the field $\mathbf{B}_0$ is equal to 15°. The changes in the ^{2}H NMR spectra are observed at temperatures close to 417 K. A single doublet with extremely narrow components appears instead of the dipole-broadened NMR lines assigned to the deuterons of the hydrogen bonds. As the temperature increases, the intensity of the narrow lines increases, whereas the intensity of the dipole-broadened lines decreases to zero (the phase coexistence typical of first-order phase transitions). The results obtained indicate that deuterons (protons) in the superionic phase exhibit a high diffusive mobility. This leads to complete averaging of the dipole–dipole interactions of the deuterons involved in the hydrogen bonds. The central NMR lines attributed to the deuterons of the ammonium groups also change at a temperature of 417 K. The NMR quartet observed in the paraelectric phase for the given orientation transforms into a doublet with a splitting of approximately 200 Hz and a linewidth of 100 Hz for each component. Therefore, the transition to the superionic phase is accompanied by the change in the structural positions of the ammonium groups (one position instead of two structurally nonequivalent positions) and, possibly, their diffusive motion. However, the rate of this diffusion is relatively

low and cannot exceed the rate corresponding to the linewidth (~100 Hz). Consequently, the contribution of the ammonium groups to the conductivity of the AHS crystal in the superionic phase is negligible and the conductivity in this phase, as in the paraelectric phase, is completely governed by the mobility of protons involved in the hydrogen bonds.

Let us now consider structural characteristics that are important for proton transport in the AHS crystal. In the paraelectric phase, the shortest distance between the protons in equivalent positions is equal to the unit cell parameter *b* (4.61 Å). This distance exceeds the shortest distance (3.91 Å) between the positions of protons in the adjacent chains of the hydrogen bonds (Fig. 1). In the adjacent tetrahedra SeO_4, the shortest distance between the oxygen atoms, which are not involved in the formation of hydrogen bonds, is approximately equal to 3.3 Å. Moreover, protons can occupy positions, for example, between the O(3) and O(4) atoms separated by a distance of 3.18 Å. Owing to thermal vibrations (librations) of the SeO_4 groups, these distances can be even shorter. As a result, hydrogen bonds with a short lifetime can be formed between the relevant O atoms. The aforementioned structural features, the results of 2*D* ^{2}H NMR investigations, and the absence of conductivity anisotropy allow us to conclude that the main mechanism of proton transport in the paraelectric phase of the AHS crystal is associated with proton hoppings between the adjacent chains of hydrogen bonds.

A drastic increase in the conductivity of the AHS crystal at temperatures above 417 K can be caused by a jumpwise decrease in the height of potential barriers to proton diffusion and also by a disordering of the oxygen atoms of the SeO_4 groups in the superionic phase, as has been observed in $(NH_4)_3H(SeO_4)_2$ crystals [18, 19]. This assumption is confirmed by the data obtained by Dvorak *et al.* [16], who explained the overall sequence of phase transitions in the AHS crystal and its deuterated analog as the result of small distortions of the praphase with the space group of symmetry *Immm* and one formula unit per unit cell. In this phase, the Se and N atoms (the centers of the SeO_4 and NH_4 groups) occupy the special positions (0 0 0) and (1/2 1/2 0), respectively. According to [16], the space groups *Immm* and *P*2/*n* describe only an averaged symmetry of the AHS crystal. In particular, the positions of the tetrahedral groups in the praphase can have an inversion center only due to disordering of the oxygen atoms through reorientation of the SeO_4 groups. In any case, the number of possible relative positions of the oxygen atoms in the SeO_4 groups and the number of possible positions of the protons in the hydrogen bonds considerably increase compared to those in the paraelectric phase. As a consequence, the conductivity of the high-temperature phase increases jumpwise. According to the ^{2}H NMR data, all protons of the hydrogen bonds in the superionic phase are described by a sole averaged electric-field gradient tensor. This suggests a high diffusive mobility of these protons.

4. CONCLUSIONS

Thus, proton exchange between hydrogen bond chains extended along the **b** axis is the main mechanism of proton transport in the paraelectric phase of the AHS crystal. Unlike the model proposed in [1, 2], the mechanism considered above is not limited by the potential barrier to reorientation of the SeO_4 groups and does not require the simultaneous breaking of two hydrogen bonds. This mechanism makes it possible, within a unified context, to explain all the available experimental data, including macroscopic measurements of electrical conductivity. The superionic conductivity in the high-temperature phase of the AHS crystal is most likely associated with orientation disordering of the SeO_4 groups, which results in an increase in the number of sites providing proton diffusion.

It can be assumed that proton chemical exchange similar to that observed in the paraelectric phase of the AHS crystal occurs in other crystals with chains of hydrogen bonds. In this respect, it would be very interesting to carry out similar investigations with crystals characterized by another configuration of the hydrogen-bond system, especially with a $KHSeO_4$ crystal in which layers of hydrogen-bond chains alternate with layers of closed dimers consisting of SeO_4 groups [20]. At present, we are involved in such investigations.

ACKNOWLEDGMENTS

This work was supported by the Russian Foundation for Basic Research, project no. 00-15-96790.

REFERENCES

1. Yu. N. Moskvich, A. A. Sukhovsky, and O. V. Rozanov, Fiz. Tverd. Tela (Leningrad) **26**, 38 (1984) [Sov. Phys. Solid State **26**, 21 (1984)].
2. R. Blinc, J. Dolinsek, G. Lahajnar, *et al.*, Phys. Status Solidi B **123**, K83 (1984).
3. A. I. Baranov, R. M. Fedosyuk, N. M. Schagina, and L. A. Shuvalov, Ferroelectr. Lett. Sect. **2**, 25 (1984).
4. Yu. N. Ivanov, J. Totz, D. Michel, *et al.*, J. Phys.: Condens. Matter **11**, 3151 (1999).
5. J. Totz, D. Michel, Yu. N. Ivanov, *et al.*, Appl. Magn. Reson. **17**, 243 (1999).
6. I. P. Aleksandrova, O. V. Rozanov, A. A. Sukhovskii, and Yu. N. Moskvich, Phys. Lett. A **95**, 339 (1983).
7. I. P. Aleksandrova, Ph. Colomban, F. Denoyer, *et al.*, Phys. Status Solidi A **114**, 531 (1989).
8. A. A. Sukhovsky, Yu. N. Moskvich, O. V. Rozanov, and I. P. Aleksandrova, Ferroelectr. Lett. Sect. **3**, 45 (1984).
9. K. S. Aleksandrov, A. I. Kruglik, S. V. Misyul', and M. A. Simonov, Kristallografiya **25**, 1142 (1980) [Sov. Phys. Crystallogr. **25**, 654 (1980)].
10. R. V. Pound, Phys. Rev. **79** (4), 685 (1950).

11. G. V. Volkoff, H. E. Petch, and D. W. Smellie, Phys. Rev. **84**, 602 (1951).
12. Yu. N. Moskvich, O. V. Rozanov, A. A. Sukhovsky, and I. P. Aleksandrova, Ferroelectrics **63**, 83 (1985).
13. A. Abragam, *The Principles of Nuclear Magnetism* (Clarendon, Oxford, 1961; Inostrannaya Literatura, Moscow, 1963).
14. C. Schmidt, B. Blümich, and H. W. Spiess, J. Magn. Reson. **79**, 269 (1988).
15. S. Kaufmann, S. Wefing, D. Schaefer, and H. W. Spiess, J. Chem. Phys. **93**, 197 (1990).
16. V. Dvorak, M. Quilichini, N. Le Calvé, *et al.*, J. Phys. I **1**, 1481 (1991).
17. A. Onodera, A. Rozycki, and F. Denoyer, Ferroelectr. Lett. Sect. **9**, 77 (1988).
18. B. V. Merinov, M. Yu. Antipin, A. I. Baranov, *et al.*, Kristallografiya **36**, 872 (1991) [Sov. Phys. Crystallogr. **36**, 488 (1991)].
19. A. Piertaszko, B. Hilczer, and A. Pawlowski, Solid State Ionics **119**, 281 (1999).
20. J. Baran and T. Lis, Acta Crystallogr., Sect. C **C42**, 270 (1986).

Translated by O. Borovik-Romanova